

For Plant Cell and Physiology Special Issue “Plant Endomembranes”

**Syntaxin of plant proteins SYP123 and SYP132 mediate root hair tip growth in
*Arabidopsis thaliana***

Running head: Function of SYP123/132 in root hair tip growth

Correspondence should be addressed to:

Masa H. Sato
Laboratory of Cellular Dynamics,
Graduate School of Life and Environmental Sciences,
Kyoto Prefectural University, 1-5 Shimogamonakaragi-cho,
Sakyo-ku, Kyoto, 606-8522, Japan
Tel/Fax: +81-75-703-5448
E-mail: mhsato@kpu.ac.jp

Subject Areas: Membrane and transport

Number of black and white figures:

Number of color figures: 8

Number of tables: 0

Type and number of supplementary materials

Supplementary figures: 7

Supplementary tables: 1

**Syntaxin of plant proteins SYP123 and SYP132 mediate root hair tip growth in
*Arabidopsis thaliana***

Mie Ichikawa^{1,7}, Tomoko Hirano^{1,2,7}, Kazuhiko Enami^{1,7}, Taylor Fuselier³, Naohiro Kato³,
Chian Kwon^{4,6}, Boris Voigt⁵, Paul Schulze-Lefert⁴, František Baluška⁵, Masa H. Sato¹

Running head: Function of SYP123/132 in root hair tip growth

1. Department of Life and Environmental Sciences, Kyoto Prefectural University, Shimogamonakaragi-cho 1-5, Sakyo-ku, Kyoto, 606-8522, Japan

2. Department of Applied Biology, Kyoto Institute of Technology, Kyoto, 606-8585, Japan

3. Department of Biological Sciences, Louisiana State University, 226 Life Science Building, Baton Rouge, LA 70803-1715, USA

4. Department of Plant Microbe Interactions, Max-Planck-Institut für Züchtungsforschung, Carl-von-Linné-Weg 10, D-50829 Köln, Germany

5. Department of Plant Cell Biology, Institute of Cellular and Molecular Botany, University of Bonn, Kirschallee 1, D-53115 Bonn, Germany

6. Department of Integrated Molecular Sciences, Dankook University, Yongin 448-701, Korea

7. These authors contributed equally to this work.

Abbreviations used are: amiRNA, artificial microRNA; ARF-GEFs, exchange factors for ARF GTPases; BFA, brefeldin A; CLSM, confocal laser scanning microscopy; FRAP, Fluorescence recovery after photo-bleaching; GFP, green fluorescent protein; GST, glutathione-S-transferase;

HA, hemagglutinin; LatB, latrunculin B; PM, plasma membrane; RFP, red fluorescent protein; RT-PCR, reverse transcriptase polymerase chain reaction; SLC, split luciferase complementation; SNARE: Soluble N-ethylmaleimide-sensitive factor attachment protein receptors; SYP, Syntaxin-of-Plant; TGN, trans-Golgi network; VAMP, vesicle-associated membrane protein; WT, wild-type

Abstract

Root hairs are fast-growing tubular protrusions on root epidermal cells that play important roles in water and nutrient uptake in plants. The tip-focused polarized growth of root hairs is accomplished by the secretion of newly synthesized materials to the tip via the polarized membrane trafficking mechanism. Here, we report the function of two different types of plasma membrane (PM) Qa-SNAREs, SYP123 and SYP132, in the growth of root hair in *Arabidopsis*. We found that SYP123, but not SYP132, localizes in the tip region of root hairs by recycling between the BFA-sensitive endosomes and the PM of the expanding tip in an F-actin-dependent manner. VAMP721/722/724 also exhibited tip-focused localization in root hairs and formed ternary SNARE complexes with both SYP123 and SYP132. These results demonstrate that SYP123 and SYP132 coordinate to mediate tip-focused membrane trafficking for root hair tip growth.

Keywords

Arabidopsis, Cell polarity, Membrane traffic, SNARE, Root hair cells

Introduction

Cell polarity is central to establishing cell morphology in eukaryotes. In plants, protrusions called root hair rapidly and characteristically extend from root hair cells. This type of tip-focused growth, called ‘tip growth’, requires polarization of the cytoplasm and unidirectional membrane trafficking to the tip region. During root hair development, newly synthesized proteins, lipids, and cell wall materials are delivered to the plasma membrane (PM) of the tip region by polarized vesicle trafficking with subsequent retrieval of excess proteins and membranous materials from the adjacent region of the tip by the endocytic pathway (Carol and Dolan 2002). The internalized materials are sorted in endosomes and partially recycled back to the tip. This complicated polarized membrane trafficking in root hair cells is established by various molecules involved in membrane trafficking, including small GTPases of the Rop, Rab, and Arf families, as well as their regulatory proteins (Molendijk et al. 2001, Xu and Scheres 2005, Preuss et al. 2004).

Soluble N-ethylmaleimide-sensitive factor attachment protein receptors (SNAREs) are essential molecules in membrane trafficking and constitute a large superfamily in eukaryotes (Hong 2005). SNAREs are categorized into two distinct classes according to their conserved residues within the SNARE motif: Q-SNARE and VAMP/R-SNARE. Q-SNARE proteins are further subdivided into three subfamilies: Qa-, Qb-, and Qc-SNAREs. Three Q-SNAREs on a

target membrane and one VAMP/R-SNARE on transport vesicles form a ternary SNARE complex for membrane fusion (Fasshauer et al. 1998). More than 60 SNARE genes have been reported for the *Arabidopsis* genome, and many *Arabidopsis* SNAREs localize on the PM (Sanderfoot 2007). In particular, nine Qa-SNARE molecules localize to the PM (Uemura et al. 2004), implying that each PM Qa-SNARE molecule has specialized physiological functions in *Arabidopsis*. Among these PM Qa-SNAREs, KNOLLE/SYP111 is predominantly expressed during mitosis and functions in cell plate formation (Lauber et al. 1997). SYP121/PEN1/SYR1 has multiple functions in various physiological steps, including accurate secretion and changes in the mobility of the KAT1 K⁺-channel (Sutter et al. 2006), and non-host resistance against powdery mildew (Collins et al. 2003). SYP122 has redundant functions with SYP121 in growth and development because the *syp121syp122* double mutant is severely dwarfed and necrotic (Assaad et al. 2004). SYP132 orthologs in *Nicotiana benthamiana* and *Medicago truncatula* play important roles in bacterial defense (Kalde et al. 2007) and symbiosome definition (Catalano et al. 2007), respectively. However, no SNARE has been reported to be involved in root hair development, although several SNARE molecules are expressed in root hair cells (Enami et al. 2009).

In contrast to the complexity of the PM Qa-SNAREs, a few R-SNARE/VAMP proteins localize to the PM in *Arabidopsis* (Uemura et al. 2004). Among the PM VAMPs, VAMP721

and VAMP722 share 96% amino acid sequence identity (Collins et al. 2003, Kwon et al. 2008, Yun et al. 2013). These VAMPs are proposed to operate in various secretory pathways by forming ternary SNARE complexes with PEN1/SYP121 (Kwon et al. 2008), SYP122 (Pajonk et al. 2008), KNOLLE/SYP111 (El Kasmi et al. 2013), and SYP132 (Yun et al. 2013). VAMP721/722 co-silenced plants are lethal (Kwon et al. 2008), suggesting that VAMP721 and VAMP722 have overlapping functions not only in the defense pathway, but also general secretion events by forming multiple PM Qa-SNAREs in *Arabidopsis*.

We previously reported SYP123 is predominately expressed in the root hair cells and localizes to the tip-region of growing root hair, whereas SYP132 uniformly localizes on the PM within the same cells (Enami et al. 2009). The difference in the subcellular distribution of these two Qa-SNAREs in tip-growing root hair cells implies that SYP123 and SYP132 may have different functions in polarized membrane trafficking to the tip region during root hair elongation.

Here, we report the function of SYP123 and SYP132 in the root hair elongation process in *Arabidopsis*. SYP123, but not SYP132, polarly localized to the tip region of root hairs via membrane recycling between the brefeldin A (BFA)-sensitive endosomes and the tip. Despite the different PM localization patterns of SYP123 and SYP132, loss-of-function of both SYP123 and SYP132 caused severe defects in root hair elongation. VAMP721/722/724 also exhibited

tip-focused localization in root hair cells and formed ternary SNARE complexes with both SYP123 and SYP132. These results indicate that two different PM Qa-SNARE, SYP123 and SYP132, coordinately function in root hair elongation in *Arabidopsis* by forming SNARE complexes with a PM R-SNARE, VAMP721/722/724.

Results

Loss of SYP123 and SYP132 expression impairs root hair elongation

We previously reported that one of the PM-resident Qa-SNAREs, SYP123, is predominantly expressed in root hair cells and polarly accumulates in the tip region of root hairs. Another PM-resident Qa-SNARE, SYP132, is also expressed in root hair cells (Enami et al. 2009). This unique expression pattern of two distinct SNAREs in root hair cells implies that both SYP123 and SYP132 are involved in root hair elongation and/or root hair cell development.

To investigate how SYP123 functions in root hair cell development, we obtained a T-DNA insertion line (CS488587) that has a T-DNA insertion in the first exon of the *SYP123* gene and designated the line as *syp123-1* (Fig. 1A). Semi-quantitative RT-PCR analysis did not detect *SYP123* transcript in homozygous *syp123-1* seedlings, indicating that *syp123-1* is a null mutant. Expression of *SYP123* was detected in a complementation line expressing GFP-SYP123 under the control of the *SYP123* promoter (Fig. 1B). The root hair length of *syp123-1* was significantly shorter ($377.2 \pm 113.8 \mu\text{m}$) than that of WT plants ($497.4 \pm 104.3 \mu\text{m}$). The expression of GFP-SYP123 under the control of the *SYP123* promoter in *syp123-1* significantly complemented the short root hair phenotype of *syp123-1*, suggesting that GFP-SYP123 is

functional (Fig. 1C, D). No difference in root length was observed between WT and *syp123-1* (Supplementary Fig. S1). Thus, only the root hair length was shortened in the *syp123-1* mutant.

Next, we investigated the function of SYP132 in root hair development. Because SYP132 is ubiquitously expressed in all tissues including root hair cells as the most conventional PM-SNARE in *Arabidopsis*, is possibly involved in the general secretion event (Enami et al. 2009, Sanderfoot 2007), it might be difficult to investigate the function of SYP132 only in root hair development using T-DNA knockout lines due to lethality. Therefore, we generated artificial microRNA (amiRNA) constructs on a pER8-modified vector, pER8GWExpA7, in which the G10-90 promoter region of pER8 vector was replaced by the *Arabidopsis* Expansin A7 promoter, which is able to conditionally induce gene expression only in root hair cells. Adding 10 μ M estradiol induced GFP only in the root hair cells of the transgenic plant generated by the vector (Supplementary Fig. S2A). After conditional induction of RNA interference of *SYP132* in the presence of estradiol, SYP132 RNA content decreased significantly in SYP132 amiRNA lines #1 and #2 (Fig. 2A and Supplementary Fig. S2B). Next, we crossed the GFP-SYP132-expressing line and the SYP132 amiRNA line to investigate whether the expression of GFP-SYP132 decreases only in root hair cells. As shown in Supplementary Fig. S2C, the fluorescence of GFP-SYP132 was strongly attenuated in root hair cells. The GFP-SYP132 fluorescence was also decreased in the non-root hair cells, probably

because of leaky expression of SYP132 amiRNA into the non-root hair cells. The length of root hairs on *SYP132* amiRNA plants was drastically shortened in the presence of estradiol in both the transgenic lines, #1 and #2 (Fig. 2 B, C). The root length in *SYP132* amiRNA plants was also decreased in the presence of estradiol, probably due to the reduced expression of SYP132 in root epidermal cells, including root hair cells and non-root hair cells (Supplementary Fig. S3). Taken together, these results clearly demonstrate that both SYP123 and SYP132 function in the root hair elongation process in *Arabidopsis*.

Focal accumulation of SYP123 in the tip region of the root hair is F-actin dependent

Because the actin cytoskeleton is known to be involved in the polarized delivery of secretory vesicles to the root hair apex (Smith and Oppenheimer 2005), we tested the effect of an actin polymerization inhibitor, latrunculin B (LatB), on the focal accumulation of GFP-SYP123 in the root hair tip. As shown in Fig. 3A and 3B, LatB treatment gradually reduced the fluorescence intensity of GFP-SYP123 in the root hair region, but no difference was found in the root hair cell region. After 30 min of treatment, the focal accumulation of GFP-SYP123 in the root hair tip completely disappeared, and little difference was observed in fluorescence intensity between the root hair region and root hair cell region. Therefore, the accumulation of GFP-SYP123 in

the root hair tip region was F-actin dependent. The localization and intensity of GFP-SYP132 on the PM of root hair was unchanged with LatB treatment (Supplementary Fig. S4).

The tip-focused distribution of GFP-SYP121 was also observed when GFP-SYP121 was expressed ectopically under the control of the CaMV 35S promoter (Supplementary Fig. S5A-D), although no fluorescence of GFP-SYP121 was observed in root hair cells when expressed under the control of its own promoter (Enami et al. 2009). The characteristic tip-focused GFP-SYP121 localization disappeared with the treatment of another actin polymerization inhibitor, cytochalasin D. The vesicles were still concentrated in the tip region after treatment (Supplementary Fig. S5E, F). Thus, SYP121 potentially localizes to the tip of root hair, and this focused accumulation of GFP-SYP121 was also F-actin dependent. Because disruption of SYP121 function caused no particular difference in root hair elongation (data not shown) and SYP121 is expressed at lower levels in root hair cells (Enami et al. 2009), the accumulation of GFP-SYP121 in the root hair tip may be an artificial effect of the ectopic expression of GFP-SYP121 under the control of the CaMV35S promoter.

SYP123, but not SYP132, is focally delivered to the root hair tip region

To test whether SYP123 is polarly delivered to the tip region of root hair, we photo-bleached pre-existing GFP-SYP123 in the root hair and analyzed the recovery of fluorescence at the PM

of root hair cells. Fluorescence recovery after photo-bleaching (FRAP) analysis showed that GFP fluorescence first recovered in the tip region of the growing root hair (Fig. 4A, C). In contrast, the tip-focused fluorescence of GFP-SYP123 was never observed in non-elongating root hair (Supplementary Fig. S6). In addition, treatment with tyrphostin A23, a well-characterized inhibitor of the clathrin-mediated endocytic pathway (Banbury et al. 2003), resulted in the disappearance of the focal accumulation of GFP-SYP123 in the root hair tip. After 60 min of treatment, the tip region of the root hair finally ruptured (Supplementary Fig. S7). These results did not occur with the non-functional analog tyrphostin A51, suggesting that clathrin-mediated endocytosis is required for the accumulation of SYP123 in the root hair tip.

In contrast to GFP-SYP123, fluorescence recovery of GFP-SYP132 was almost identical between the tip and base regions of the root hair (Fig. 4B, D), suggesting that the distribution of SYP132 in the tip region of the root hair cells is not polar.

Brefeldin A induces large aggregated GFP-SYP123 structures inside the root hair region

BFA is known to interfere with the recycling of several PM proteins, inhibiting the activity of the exchange factors for ARF GTPases (ARF-GEFs) and forming large aggregations called “BFA compartments” inside cells (Satiat-Jeunemaitre et al. 1996, Staehelin and Driouich 1997).

We treated the growing root hair cells of transgenic plants expressing GFP-SYP123 and GFP-

SYP132 with BFA to test whether the treatment affects the localization of these SNAREs.

Although no change in the localization pattern was observed in the control experiment (Fig. 5A), after 30 min of BFA treatment a few large GFP-SYP123 aggregations were observed in the root hair cells, particularly in the root hair region. GFP-SYP123 was completely depolarized from the PM of the root hair tip, and GFP-SYP123 became uniformly distributed to the entire PM of the root hair cells (Fig. 5B). The tip-focused localization of ectopically expressed GFP-SYP121 in growing root hairs also exhibited a strong response to BFA. After 30 min, the tip-polarization of GFP-SYP121 completely disappeared and large aggregations of GFP fluorescence emerged inside of the root hair (Supplementary Fig. S5G). In contrast, no change in localization or aggregation of GFP-SYP132 was observed after 30 min of BFA treatment (Fig. 5C, D). These data strongly suggest that the polarized distribution of SYP121 and SYP123, but not SYP132, in the root hair tip is BFA-sensitive.

SNARE complex formation by SYP123, SYP132, and VAMP721/722/724

Most of the VAMP72 family proteins (e.g., VAMP721, VAMP722, VAMP724, VAMP725, and VAMP726), except VAMP727, localize to the PM (Uemura et al. 2004, Ueda et al. 2004). Among the PM-localized VAMP72 proteins, VAMP721/722 have been proposed to function in various exocytic pathways by forming distinct SNARE complexes with PEN1/SYP121 (Kwon

et al. 2008), KNOLLE (El Kasmi et al. 2013), and SYP123 (Yun et al. 2013), implying that VAMP72s also form SNARE complexes with SYP123 in root hair cells. Microarray analysis using the *Arabidopsis* eFP Browser program (Winter et al. 2007) revealed that VAMP721, VAMP722, and VAMP724 are expressed in the root tissues. To determine which VAMP72s are expressed in root hairs, we generated transgenic plants expressing mRFP-VAMP721, -VAMP722, and -VAMP724 under the control of their promoters. As shown in Fig. 6, mRFP-VAMP721/722/724 were expressed in root hair cells and accumulated in the root hair tip region. This accumulation disappeared and a few large aggregations formed after BFA treatment (Fig. 6B, D, F), indicating that the focal accumulation of VAMP72s in the root hair tip is a BFA-sensitive recycling process.

Next, we tested the possibility of *in vitro* ternary SNARE complex formation by SYP123 and SNAP33 with various VAMP72 proteins. Each VAMP72 protein (i.e., VAMP721, VAMP722, VAMP724) was incubated with recombinant HA-tagged SYP123 (HA-SYP123) and glutathione-S-transferase (GST)-fused SNAP33 (GST-SNAP33). Protein complexes were recovered by the adsorption of GST-SNAP33 to glutathione Sepharose 4B and analyzed for the presence of SDS-resistant ternary SNARE complexes by immunoblot analysis with the anti-HA antibody. The high molecular weight bands disappeared with boiling, indicating that SYP123 might form SDS-resistant ternary SNARE complexes with all VAMP72 proteins (i.e.,

VAMP721, VAMP722, and VAMP724) tested *in vitro* (Fig. 7A). These results suggest that SYP123 potentially has an ability to form ternary SNARE complexes with SNAP33 and various VAMP72 proteins *in vitro*.

To confirm the interaction between SYP1s and VAMP72s, we also examined the *in vivo* interaction of SYP121, SYP123, and SYP132 with VAMP72s using the split luciferase complementation (SLC) assay (Fujikawa and Kato 2007). In the SLC assay, a protein pair of interest is genetically fused to the N- or C-terminal fragment of *Renilla* luciferase (Nluc or Cluc, respectively) and transiently expressed in *Arabidopsis* protoplasts. The interaction of the protein pairs is then evaluated by measuring complemented luciferase activities. We successfully demonstrated in a previous study that the SCL assay allows the evaluation of binary interactions among various SNARE subfamilies (Kato et al. 2010). Therefore, we transiently expressed three distinct SYP1s (Nluc-SYP121, Nluc-SYP123, or Nluc-SYP132) and four distinct VAMP72s (Cluc-VAMP721, Cluc-VAMP722, Cluc-VAMP723, and Cluc-VAMP724) simultaneously in *Arabidopsis* protoplasts to evaluate the interaction of SYP121, SYP123, and SYP132 with VAMP72s. As shown in Fig. 7B, strong interactions were observed between SYP1s and the PM-localized VAMP72s (i.e., VAMP721, VAMP722, and VAMP724). No or little interaction was observed with the TGN-localized SYP41/vacuolar-localized SYP22 pair used as a negative control (Fujikawa and Kato 2007) or the PM-localized SYP1s and ER-localized VAMP723 pair.

Taken together, these results suggest that SYP123 and SYP132 in the PM form SNARE complexes with VAMP721/722/724 with no difference in interaction specificity in *Arabidopsis* root hair cells.

Discussion

We previously reported that both SYP123 and SYP132 are expressed in root hair cells with different localization patterns: SYP123 is predominantly expressed in root hair cells and accumulates in the root hair tip, whereas SYP132 is ubiquitously expressed in all tissues and uniformly localizes to the PM (Enami et al. 2009). These results imply that these two PM-SNAREs may be coordinately involved in the development of root hair cells.

In the present study, we examined how these PM-SNAREs contribute to root hair elongation in *Arabidopsis*. Impairing the function of SYP123 and SYP132 individually strongly inhibited root hair elongation, suggesting that both SYP123 and SYP132 function on the membrane trafficking cell surface materials during root hair elongation, despite SYP123 and SYP132 having different localization patterns in root hair cells.

Disruption of the tip-focused accumulation of GFP-SYP123 by LatB treatment suggests that the polar localization of SYP123 is achieved by the actin cytoskeleton. Intriguingly, GFP-SYP121 also accumulates in the tip region of the root hair when the protein is ectopically

expressed in root hair cells. SYP121 is known to be focally recruited to the fungal penetration site for deposition of cell wall materials for papilla formation (Assaad et al. 2004, Bhat et al. 2005). Alternatively, SYP12 family proteins SYP124 and SYP125 predominantly localize to the tip region of growing pollen tubes (Enami et al. 2009, Silva et al. 2010, Ul-Rehman et al. 2011), and transiently expressed GFP-SYP121, GFP-SYP122, and GFP-SYP124 in tobacco exhibit focal accumulation in the tip region of pollen tubes (Silva et al. 2010). Upon fungal infection, actin microfilaments become focused on the penetration site (Takemoto et al. 2006, Shimada et al. 2006). In growing root hairs and pollen tubes, actin cytoskeleton functions not only in organelle movement, but also in polarized secretion of cell wall and membranous materials (Carol and Dolan 2002, Šamaj et al. 2006). A high similarity in amino acid sequences and gene structures among SYP12 family proteins indicate that all SYP12 family proteins potentially have the ability to interact with the F-actin cytoskeleton in order to focally accumulate in particular domains on the PM. Future studies need to confirm the interaction between actin and SYP12s and the actin interaction domain of SYP12s.

One important role of the actin cytoskeleton in promoting tip growth in root hair or pollen tubes is to drive the long-range movement of secretory vesicles, transporting cell wall and plasma membrane materials toward the tip (Smith and Oppenheimer 2005). A plant homolog of mammalian RAB11 in *Arabidopsis*, RabA4b, localizes to the clear zone of growing

root hair (Preuss et al. 2004). This localization depends on an intact actin cytoskeleton, and the tip-focused localization of RabA4b is essential for sustained growth of the root hair tip. The Rab protein acts as a molecular switch in membrane trafficking by cycling between active GTP-bound and inactive GDP-bound states. The RABs activated by the guanine nucleotide exchange factor (GEF) tether transport vesicles to the target organelle membrane, and SNAREs function in the subsequent step of vesicle and target membrane fusion (Ueda et al. 2012). Therefore, the tip-focused accumulation of SYP123 may indicate that SYP123 and RabA4b are cooperatively involved in root hair elongation.

BFA is known to inhibit the secretion process to perturb ARF-GEFs in eukaryotes (Klausner et al. 1992). In plants, BFA treatment results in the so-called BFA compartments, which are composed of TGN/early endosomes and inhibit a wide variety of membrane trafficking events (Satiat-Jeunemaitre et al. 1996). Various tropic responses and development are controlled by directional auxin flow, which is mainly established by polar localization of auxin transporters, such as AUX1, PGP, and PIN (Swarup et al. 2001, Terasaka et al. 2010, Feraru and Friml 2008). In particular, the polarity of PIN family proteins are established by the endocytic recycling pathway, which is controlled by the BFA-sensitive ARF-GEF GNOM (Geldner et al. 2003, Kleine-Vehn et al. 2008). In root hairs, BFA-induced aggregations of early endosomes are formed in the presence of BFA and root hair elongation is completely inhibited

(Ovecka et al. 2005, Hlavacka et al. 2005, Ovecka et al. 2010). Similarly, we found that BFA treatment results in a few large aggregations and the depolarization of GFP-SYP123 and mRFP-VAMP721/722/724, but not GFP-SYP132, in root hair cells. These findings suggest that the polarized localization of SYP123 and mRFP-VAMP72s is accomplished by the BFA-sensitive membrane recycling mechanism in root hair cells.

The proteins of the PM-localized SYP1 Qa-SNARE family have different spatio-temporal expression patterns: SYP132 is expressed ubiquitously in all tissues throughout plant development, whereas SYP124, SYP125, and SYP131 are only expressed in pollen, and SYP123 appears to be exclusively expressed in root hair cells during root development (Enami et al. 2009). KNOLLE/SYP111 is a specialized SYP1 syntaxin in flowering plants that is required for cytokinesis (Lauber et al. 1997). SYP121/PEN1/SYR1 is reported to be involved in various physiological processes, including secretion, cellular growth (Geelen et al. 2002), ion homeostasis (Leyman 1999), and non-host resistance to powdery mildew fungus (Collins et al. 2003). SYP122, a paralog of SYP121, is phosphorylated in response to elicitor flagellin (Nühse et al. 2003). A *syp121syp122* double mutant previously exhibited a dwarfed and necrotic phenotype, suggesting that these two PM SNARE molecules have redundant functions not only in plant immunity, but also in general secretion events (Assaad et al. 2004, Zhang et al. 2007). SYP132 is ubiquitously expressed in *Arabidopsis* (Enami et al. 2009) and has been related to

the most ancient evolutionary branch of SYP1 proteins (Reichardt et al. 2011), suggesting that SYP132 is involved in the general secretion event in land plants. Although no function has been reported so far for SYP132 in *Arabidopsis*, SYP132 orthologs play important roles in bacterial defense in *Nicotiana benthamiana* (Kalde et al. 2007) and symbiosome membrane definition in *Medicago truncatula* (Catalano et al. 2007). Therefore, these results suggest that PM-resident Qa-SNARE molecules function in different membrane trafficking pathways leading to particular domains or the entire PM for the transport of various functional molecules in a polarized or non-polarized manner. In contrast to the complexity of SYP1s, basically only one type of VAMP/R-SNARE exists; VAMP721/722 forms SNARE complexes with various SYP1 molecules in vegetative tissues (Lipka et al. 2007, Yun et al. 2013, Kato et al. 2010). Recently, KNOLE/SYP111 is reported to interact with NPSN (Qb) and SYP7 (Qc) instead of SNAP33 (Qb + Qc) (El Kasmi et al. 2013), suggesting that two different types of PM-SNARE complex are generated during the membrane fusion between secretory vesicles and the PM. Although we found no clear difference in the interaction specificity of VAMP721/722/724 with SYP123 or SYP132 in our experimental conditions, two different types of SNARE complex may form between SYP123/132 and VAMP721/722/724 to interact with distinct types of the PM Qb- and Qc-SNAREs in root hair elongation process.

. In conclusion, we propose that *de novo* secretion of cell wall and plasma membrane materials is established by a SYP132 and VAMP721/722/724-mediated non-polar secretory pathway, and that secretory vesicles are then recycled by the clathrin-dependent endocytic and BFA-sensitive exocytic pathway and focally delivered to the root hair tip by a SYP123 and VAMP721/722/724-mediated vesicle fusion process. Consequently, tip-focused polarized secretion is established in root hair cells (Fig. 8).

Materials and Methods

Plant material and growth conditions

The *syp123-1* T-DNA insertion mutant line CS488587 (*Arabidopsis thaliana* ecotype Columbia background) was obtained from the Arabidopsis Biological Resource Center (ABRC). The inserted locus was sequence-verified by analysis of the PCR-amplified fragment using appropriate primer sets. Establishment of the GFP-SYP123 and GFP132 lines and the growth conditions were reported previously (Enami et al. 2009).

Plasmid construction and plant transformation

For the construction of estrogen-induced artificial microRNA (amiRNA) SYP132 and GFP constructs, the pER8 vector (Zuo et al. 2000) was digested with SpeI and XhoI and then blunted by the T4 DNA polymerase. The Gateway conversion cassette (Invitrogen) was ligated into the blunted vector. The resulting vector was designated pER8GW. The G10-90 promoter of pER8GW was replaced by the *Arabidopsis* Expansin A7 promoter sequence to generate pER8GWExpA7. To generate the SYP132 amiRNA construct for inhibition of SYP132 expression, we designed an optimal amiRNA sequence using the WMD3 program (<http://wmd3.weigelworld.org/cgi-bin/webapp.cgi>). The designed target 21-mer amiRNA

sequence (5'-TGTTACTGTATAAAGTCGCCT-3') was synthesized using the following primers: (miRNA-sense, miRNA-antisense, miRNA*-sense, miRNA*-antisense, see supplementary table1) according to the method described by Ossowski et al. (2008). GFP and SYP132 amiRNA sequences were subcloned into pER8GWExpA7 using the Gateway cloning method according to the manufacturer's instructions.

P_{AtVAMP72s}::mRFP-AtVAMP72s (721, 722, 724) were constructed using the FTFLP method described previously (Ebine et al. 2011). *Agrobacterium tumefaciens* strain *GV3101* was used for transformation into plants by the floral dip method (Clough and Bent 1998).

For the *in vitro* SNARE complex assay, cDNAs corresponding to SYP123, AtVAMP72s, and AtSNAP33 were obtained by RT-PCR using *Arabidopsis* RNA extracts or from RIKEN. The full-length coding regions were amplified by PCR and sub-cloned into the plasmid vector pGEX-6p-1 (GE Health). The HA tag was fused with SYP123 by adding corresponding DNA sequences to primers for PCR.

RT-PCR

Total RNA was extracted using the RNeasy plant mini kit (QIAGEN) according to the manufacturer's instructions. First strand cDNAs were synthesized using an RNA PCR kit

(Takara Bio) with oligo-dT primer. The cDNA was amplified by PCR using a set of primers specific to *SYP123* or *ACT2*. PCR products were loaded on 1.0% agarose gel.

Inhibitor treatment

For the inhibitor assay, 4d-old seedlings were submerged into 1 ml of distilled water containing the respective inhibitor or corresponding amount of solvents in microtubes, and then subjected to microscopy. In the case of the time lapse chase assay, seedlings were directly mounted on a glass slide in the presence of a working solution of the inhibitor and monitored. The final concentration and duration of each inhibitor treatment was as follows: 2 μ M latrunculin B (Calbiochem) for 30 min, 20 μ M brefeldin A (Sigma) and 50 μ M tyrphostin A23 and A51 (Sigma) for 1 h.

Confocal microscopy and image analysis

Fluorescent signals and corresponding differential interference contrast (DIC) values were obtained using a Nikon ECLIPSE E600 laser scanning microscope equipped with a C1si-ready confocal system (Nikon, Tokyo, Japan), an argon laser, and a green HeNe laser. The collected images were processed using Nikon EZ-C1 software and analyzed using ImageJ 1.38X.

For FRAP analysis, transgenic plants were cultivated on cover slips with 1/2 MS medium. After 5d, the cover glasses with seedlings were inverted on glass slides, and put on the stage of the microscope for CLSM. FRAP experiments were performed using a laser-scanning microscope (Eclipse E600; Nikon) equipped with the C1-si ready confocal system (Nikon). Bleaching was carried out on the root hair with the laser power set to 100% until the GFP fluorescence was bleached. The images were obtained at 5 minutes intervals for 30 minutes and analyzed using EZ-C1 software (Nikon) to measure GFP intensity.

In vitro SNARE complex assay

To express SNARE proteins in bacteria, the plasmid DNA constructs mentioned above were transformed into the *E. coli* BL21 (DE3) *pLysS* strain. Protein expression was induced by adding 1 mM IPTG to the bacterial suspension and the expressed recombinant proteins affinity-purified using glutathione-Sepharose 4B (GE Health). To obtain the GST-devoid proteins, bead-bound proteins were digested with PreScission Protease (GE Health) and the released proteins were collected. To analyze ternary SNARE complex formation, equimolar (1 μ M) amounts of protein were mixed and incubated at 4°C overnight. After retrieving the interacting proteins by precipitating GST-SNAP33 with glutathione Sepharose 4B, the matrix-bound complexes were subjected to immunoblot analysis using anti-HA and anti-GST antibodies. To detect SDS-

resistant but heat-labile ternary SNARE complexes, boiled and non-boiled protein samples were compared.

Split luciferase complementation assay

The split luciferase complementation assay was performed as reported previously (Kato and Bai 2010). Briefly, protoplasts were prepared from the rosette leaves of 3 to 4-week-old *Arabidopsis thaliana* Col-0 plants. The protoplasts were then transformed in 96-well microplates with equal amounts of the pDuExAn6 and pDuExD7 plasmids expressing full-length cDNAs of interest (Fujikawa and Kato 2007). In the plasmids, the cDNA was inserted into the C-terminal end of the sequence that encodes either the N- or C-terminal fragment of *Renilla* luciferase. To measure the complemented *Renilla* luciferase activities, luminescence was detected by a microplate luminometer after adding ViviRen (Promega), a *Renilla* luciferase substrate, to protoplast solutions in the wells. To normalize for deviations in the transformation efficiency in each well, the protoplasts were co-transformed with the pMONT plasmid expressing click beetle red luciferase (Kato et al. 2010). The click beetle red luciferase-dependent luminescence was measured after adding luciferin, a click beetle red luciferase substrate, to the protoplast solutions in the wells. Because luciferin and ViviRen emit different colors of fluorescence (red and cyan, respectively), the click beetle luciferase-dependent luminescence was detected

through a red filter (Kodak Wratten filter No. 29, Kodak) after measuring the *Renilla* luciferase-dependent luminescence. The *Renilla* luciferase-dependent luminescence was expressed in normalized relative luminescence units (nRLUs) and calculated by dividing the cyan luminescence unit by the red luminescence unit.

Funding information

This work was supported by a Grant-in-Aid for Basic Science Research (C) and a Grant-in-Aid for Scientific Research on Innovative Areas (No. 25119720) from the Japanese Ministry of Education, Culture, Sports, Science and Technology and the Strategic Research Funds of Kyoto Prefectural University to M.H.S., and Grants in-Aid to M. I. and K. E. for Scientific Research for Plant Graduate Students from Nara Institute of Science and Technology, supported by The Ministry of Education, Culture, Sports, Science and Technology, Japan.

Acknowledgements

We thank T. Aoyama (Kyoto University, Japan) and T. Nakagawa (Shimane University, Japan) for providing the *Arabidopsis* Expansin A7 construct and pGWB vectors, respectively. We also thank K. Tamura (Kyoto University, Japan) for technical assistance with confocal microscopy.

Disclosures

No conflicts of interest declared.

References

- Assaad, F.F., Qiu, J., Youngs, H., Ehrhardt, D., Zimmerli, L., Kalde, M., Wanner, G., Peck, S.C., Edwards, H., Ramonell, K., Somerville, C.R., Thordal-Christensen, H. (2004) The PEN1 Syntaxin Defines a Novel Cellular Compartment Assembly of Papillae. *Mol. Biol. Cell* 15: 5118–5129.
- Banbury, D. N., Oakley, J.D., Sessions, R.B., Banting, G. (2003) Tyrphostin A23 inhibits internalization of the transferrin receptor by perturbing the interaction between tyrosine motifs and the medium chain subunit of the AP-2 adaptor complex. *J. Biol. Chem.* 278: 12022-12028.
- Bhat, R.A., Miklis, M., Schmelzer, E., Schulze-lefert, P., and Panstruga, R. (2005) Recruitment and interaction dynamics of plant penetration resistance components in a plasma membrane microdomain. *Proc. Natl. Acad. Sci. USA* 102: 3135–3140.
- Carol, R.J. and Dolan, L. (2002) Building a hair: tip growth in *Arabidopsis thaliana* root hairs. *Philos. Trans. R. Soc. Lond. B Biol. Sci.* 357: 815–821.
- Catalano, C.M., Czymmek, K.J., Gann, J.G., and Sherrier, D.J. (2007) *Medicago truncatula* syntaxin SYP132 defines the symbiosome membrane and infection droplet membrane in root nodules. *Planta* 225: 541–550.

- Clough, S.J. and Bent, A.F. (1998) Floral dip: a simplified method for *Agrobacterium*-mediated transformation of *Arabidopsis thaliana*. *Plant J.* 16: 735–743.
- Collins, N.C., Thordal-christensen, H., and Lipka, V. (2003) SNARE-protein-mediated disease resistance at the plant cell wall. *Nature* 312: 973-977.
- Ebine, K., Fujimoto, M., Okatani, Y., Nishiyama, T., Goh, T., Ito, E., Dainobu, T., Nishitani, A., Uemura, T., Sato, M.H., Thordal-Christensen, H., Tsutsumi, N., Nakano, A., Ueda, T. (2011) A membrane trafficking pathway regulated by the plant-specific RAB GTPase ARA6. *Nat. Cell Biol.* 13: 853–859.
- Enami, K., Ichikawa, M., Uemura, T., Kutsuna, N., Hasezawa, S., Nakagawa, T., Nakano, A., and Sato, M.H. (2009) Differential expression control and polarized distribution of plasma membrane-resident SYP1 SNAREs in *Arabidopsis thaliana*. *Plant Cell Physiol.* 50: 280–289.
- Fasshauer, D., Sutton, R.B., Brunger, a T., and Jahn, R. (1998) Conserved structural features of the synaptic fusion complex: SNARE proteins reclassified as Q- and R-SNAREs. *Proc. Natl. Acad. Sci. USA.* 95: 15781-15786.
- Feraru, E. and Friml, J. (2008) PIN polar targeting. *Plant Physiol.* 147: 1553-1559.

- Fujikawa, Y. and Kato, N. (2007) Split luciferase complementation assay to study protein-protein interactions in *Arabidopsis* protoplasts. *Plant J.* 52: 185-195.
- Geelen, D., Leyman, B., Batoko, H., Sansabastiano, G. Di, Moore, I., and Blatt, M.R. (2002) The abscisic acid-related SNARE homolog NtSyr1 contributes to secretion and growth□: evidence from competition with its cytosolic domain. *Plant Cell* 14: 387-406.
- Geldner, N., Anders, N., Wolters, H., Keicher, J., Kornberger, W., Muller, P., Delbarre, A., Ueda, T., Nakano, A., and Jürgens, G. (2003) The *Arabidopsis* GNOM ARF-GEF mediates endosomal recycling, auxin transport, and auxin-dependent plant growth. *Cell* 112: 219-230.
- Hlavacka, A., Voigt, B., Timmers, A.C.J., Jozef, S., Ueda, T., Preuss, M., Nielsen, E., Mathur, J., Emans, N., Stenmark, H., Nakano, A., and Menzel, D. (2005) Actin-based motility of endosomes is linked to the polar tip growth of root hairs. *Eur. J. Cell Biol.* 84: 609-621.
- Hong, W. (2005) SNAREs and traffic. *Biochim. Biophys. Acta* 1744: 120-144.
- Kalde, M., Nu, T.S., Findlay, K., and Peck, S.C. (2007) The syntaxin SYP132 contributes to plant resistance against bacteria and secretion of pathogenesis-related protein 1. *Proc. Natl. Acad. Sci. USA* 104: 11850-11855.

- El Kasmi, F., Krause, C., Hiller, U., Stierhof, Y.-D., Mayer, U., Conner, L., Kong, L., Reichardt, I., Sanderfoot, A. a, and Jürgens, G. (2013) SNARE complexes of different composition jointly mediate membrane fusion in *Arabidopsis* cytokinesis. *Mol. Biol. Cell* 24: 1593-1601.
- Kato, N. and Bai, H. (2010) Expression, localization and interaction of SNARE proteins in *Arabidopsis* are selectively altered by the dark. *Plant Signal. Behav.* 5: 1470-1472.
- Kato, N., Fujikawa, Y., Fuselier, T., Adamou-Dodo, R., Nishitani, A., and Sato, M.H. (2010) Luminescence detection of SNARE-SNARE interaction in *Arabidopsis* protoplasts. *Plant Mol. Biol.* 72: 433-444.
- Klausner, R.D., Donaldson, J.G., and Lippincott-Schwartz, J. (1992) Brefeldin A: insights into the control of membrane traffic and organelle structure. *J. Cell Biol.* 116: 1071-1080.
- Kleine-Vehn, J., Dhonukshe, P., Sauer, M., Brewer, P.B., Wiśniewska, J., Paciorek, T., Benková, E., and Friml, J. (2008) ARF GEF-dependent transcytosis and polar delivery of PIN auxin carriers in *Arabidopsis*. *Curr. Biol.* 18: 526-531.
- Kwon, C., Neu, C., Pajonk, S., Yun, H.S., Lipka, U., Humphry, M., Bau, S., Straus, M., Kwaaitaal, M., Rampelt, H., El Kasmi, F., Jürgens, G., Parker, J., Panstruga, R., Lipka, V., Schulze-Lefert, P. (2008) Co-option of a default secretory pathway for plant immune responses. *Nature* 451: 835-840.

- Lauber, M.H., Waizenegger, I., Steinmann, T., Schwarz, H., Mayer, U., Hwang, I., Lukowitz, W., Jürgens, G. (1997) KNOLLE Protein is a cytokinesis-specific syntaxin. *J. Cell Biol.* 139: 1485-1493.
- Leyman, B. (1999) A tobacco syntaxin with a role in hormonal control of guard cell ion channels. *Science* . **283**: 537-540.
- Lipka, V., Kwon, C., and Panstruga, R. (2007) SNARE-Ware□: The Role of SNARE-Domain Proteins in Plant Biology. *Annu. Rev. Cell Dev. Biol.* 147-174.
- Molendijk, A.J., Bischoff, F., Rajendrakumar, C.S. V, Friml, Â., Braun, M., and Gilroy, S. (2001) *Arabidopsis thaliana* Rop GTPases are localized to tips of root hairs and control polar growth. *EMBO J.* 20: 2779-2788.
- Nühse, T.S., Boller, T., and Peck, S.C. (2003) A plasma membrane syntaxin is phosphorylated in response to the bacterial elicitor flagellin. *J. Biol. Chem.* 278: 45248-45254.
- Ossowski, S., Schwab, R., and Weigel, D. (2008) Gene silencing in plants using artificial microRNAs and other small RNAs. *Plant J.* 53: 674-690.
- Ovecka, M., Berson, T., Beck, M., Derksen, J., Samaj, J., Baluska, F., and Lichtscheidl, I.K. (2010) Structural sterols are involved in both the initiation and tip growth of root hairs in *Arabidopsis thaliana*. *Plant Cell* 22: 2999-3019.

- Ovecka, M., Lang, I., Baluska, F., Ismail, A., Illes, P., and Lichtscheidl, I.K. (2005) Endocytosis and vesicle trafficking during tip growth of root hairs. *Protoplasma* 226: 39-54.
- Pajonk, S., Kwon, C., Clemens, N., Panstruga, R., and Schulze-Lefert, P. (2008) Activity determinants and functional specialization of *Arabidopsis PEN1* syntaxin in innate immunity. *J. Biol. Chem.* 283: 26974-26984.
- Preuss, M.L., Serna, J., Falbel, T.G., Bednarek, S.Y., and Nielsen, E. (2004) The *Arabidopsis* Rab GTPase RabA4b Localizes to the Tips of Growing Root Hair Cells. *Plant Cell* 16: 1589-1603.
- Reichardt, I., Slane, D., El Kasmi, F., Knöll, C., Fuchs, R., Mayer, U., Lipka, V., and Jürgens, G. (2011) Mechanisms of functional specificity among plasma-membrane syntaxins in *Arabidopsis*. *Traffic* 12: 1269-1280.
- Šamaj, J., Müller, J., Beck, M., Böhm, N., and Menzel, D. (2006) Vesicular trafficking, cytoskeleton and signalling in root hairs and pollen tubes. *Trends Plant Sci.* 11: 594-600.
- Sanderfoot, A. (2007) Increases in the Number of SNARE Genes Parallels the Rise of Multicellularity among the Green Plants *Plant Physiol.* 144: 6-17.

- Satiat-Jeunemaitre, B., Cole, L., Bourett, T., Howard, R., and Hawes, C. (1996) Brefeldin A effects in plant and fungal cells: something new about vesicle trafficking? *J. Microsc.* 181: 162-177.
- Shimada, C., Lipka, V., Connell, R.O., Okuno, T., Schulze-lefert, P., and Takano, Y. (2006) Nonhost resistance in *Arabidopsis-Colletotrichum* interactions acts at the cell periphery and requires actin filament function. *Mol. Plant Microbe Interact.* 19: 270-279.
- Silva, P.A., Ul-Rehman, R., Rato, C., Di Sansebastiano, G.-P., and Malhó, R. (2010) Asymmetric localization of *Arabidopsis* SYP124 syntaxin at the pollen tube apical and sub-apical zones is involved in tip growth. *BMC Plant Biol.* 10: 179.
- Smith, L.G. and Oppenheimer, D.G. (2005) Spatial control of cell expansion by the plant cytoskeleton. *Annu. Rev. Cell Dev. Biol.* 21: 271-295.
- Staelin, L.A. and Driouich, A. (1997) Brefeldin A effects in Plants (Are Different Golgi Responses Caused by Different Sites of Action?). *Plant Physiol.* **114**: 401-403.
- Sutter, J., Campanoni, P., Tyrrell, M., and Blatt, M.R. (2006) Selective mobility and sensitivity to SNAREs is Exhibited by the *Arabidopsis* KAT1 K⁺ channel at the plasma membrane. *Plant Cell* 18: 935-954.

Swarup, R., Friml, J., Marchant, a, Ljung, K., Sandberg, G., Palme, K., and Bennett, M. (2001)

Localization of the auxin permease AUX1 suggests two functionally distinct hormone transport pathways operate in the *Arabidopsis* root apex. *Genes Dev.* 15: 2648-2653.

Takemoto, D., Jones, D.A., and Hardham, A.R. (2006) Re-organization of the cytoskeleton and

endoplasmic reticulum in the *Arabidopsis pen1-1* mutant inoculated with the non-adapted powdery mildew pathogen, *Blumeria graminis* f. sp. hordei. *Mol. Plant Pathol.* 7: 553-563.

Terasaka, K., Blakeslee, J.J., Titapiwatanakun, B., Peer, W.A., Bandyopadhyay, A., Makam,

S.N., Lee, R., Richards, E.L., Murphy, A.S., Sato, F., and Yazaki, K. (2005) PGP4 , an ATP binding cassette P-glycoprotein , catalyzes auxin transport in *Arabidopsis thaliana* roots. *Plant Cell* 17: 2922-2939.

Ueda, T., Sato, M.H., and Uemura, T. (2012) The role of RAB GTPases and SNARE proteins in

plant endocytosis and post-Golgi trafficking. In *Endocytosis in Plants*, J. Samaj, ed (Springer-Verlag, Berlin Heidelberg), pp. 201-216.

Ueda, T., Uemura, T., Sato, M.H., and Nakano, A. (2004) Functional differentiation of

endosomes in *Arabidopsis* cells. *Plant J.* 40: 783-789.

Uemura, T., Ueda, T., Ohniwa, R.L., Nakano, A., Takeyasu, K., and Sato, M.H. (2004)

Systematic analysis of SNARE molecules in *Arabidopsis*: dissection of the post-Golgi network in plant cells. *Cell Struct. Funct.* 29: 49-65.

- Ul-Rehman, R., Silva, P.Â., and Malhó, R. (2011) Localization of *Arabidopsis* SYP125 syntaxin in the plasma membrane sub-apical and distal zones of growing pollen tubes. *Plant Signal. Behav.* 6: 665-670.
- Winter, D., Vinegar, B., Nahal, H., Ammar, R., Wilson, G. V, and Provart, N.J. (2007) An “Electronic Fluorescent Pictograph” browser for exploring and analyzing large-scale biological data sets. *PLoS One* 2: e718.
- Xu, J. and Scheres, B. (2005) Dissection of *Arabidopsis* ADP-RIBOSYLATION FACTOR 1 Function in Epidermal Cell Polarity. *Plant Cell* 17: 525-536.
- Yun, H.S., Kwaaitaal, M., Kato, N., Yi, C., Park, S., Sato, M.H., Schulze-Lefert, P., and Kwon, C. (2013) Requirement of vesicle-associated membrane protein 721 and 722 for sustained growth during immune responses in *Arabidopsis*. *Mol. Cells* 35: 1-8.
- Zhang, Z., Feechan, A., Pedersen, C., Newman, M.A., Qiu, J., Olesen, K.L., and Thordal-Christensen, H. (2007) A SNARE-protein has opposing functions in penetration resistance and defence signalling pathways. *Plant J.* 49: 302-312.
- Zuo, J., Niu, Q.W., and Chua, N.H. (2000) Technical advance: An estrogen receptor-based transactivator XVE mediates highly inducible gene expression in transgenic plants. *Plant J.* 24: 265-273.

Figure legends

Fig. 1. The root hair elongation phenotype of the *syp123* mutant. (A) Schematic representation of *SYP123* gene and the position of the T-DNA insertion. Boxes indicate exons. Dark grey regions indicate untranslated regions. The open triangle indicates the position of the T-DNA insertion. Arrows indicate the positions of primers used for RT-PCR and genomic PCR. (B) RT-PCR analysis to detect the expression of *SYP123* in wild-type (WT) and mutant plants. Total RNA was purified from 7d-seedlings. *ACT2* was used as an internal control. “Genomic DNA” indicates that PCR was performed by using *Arabidopsis* genomic DNA as a template. (C) Lengths of root hairs from WT, *syp123-1* mutant, and the complementation line expressing GFP-SYP123 under the control of its promoter in *SYP123-1*. Root hair length was measured using the 10 longest root hairs from 20 primary roots of 5-day-old each seedling on half-length MS agar plates. Values represent mean \pm SD of 200 root hairs. * $p < 0.01$, t-test. (D) Images of roots from WT, *syp123-1*, and GFP-SYP123/*syp123-1* plants. Scale Bar = 500 μ m.

Fig. 2. The root hair elongation phenotype of SYP132 amiRNA plants. (A) RT-PCR analysis to detect the expression of SYP132 amiRNA plants (lines #1 and #2) and a GFP-expressing line in the presence or absence of 10 μ M estradiol. *SYP123* in wild-type (WT) and mutant plants. *ACT2*

was used as an internal control. (B) Images of roots from SYP132 amiRNA plants (lines #1 and #2) in the presence or absence of estradiol. Scale bars = 1000 μm . (C) The lengths of roots from SYP132 amiRNA plants in the presence or absence of 10 μM estradiol. Root hair length was measured using the 10 longest root hairs from 20 primary roots of 5-day-old each seedling on half-length MS agar plates. Values represent mean \pm SD of 200 root hairs. * $p < 0.01$, t-test.

Fig. 3. Effect of latrunculin B treatment on the accumulation of GFP-SYP123 in the tip region of root hair cells. (A) Reconstituted 3D projection images of serial z-stack sections of root hair cells at the indicated times. GFP-SYP123 fluorescence immediately dispersed in the tip region of root hairs upon the addition of 2 μM latrunculin B. (B) Quantitative analysis of signal intensity within the root hair cell (dotted circle) and root hair region (open circle) shown in (A). Scale bar = 20 μm

Fig. 4. FRAP analysis of GFP-SYP123 and GFP-SYP132. (A) GFP fluorescence images of GFP-SYP123 and (B) GFP-SYP132 before and after photo-bleaching. Before collecting the fluorescence images, photo-bleaching was performed around the root hair tip region. Fluorescence intensity was measured in the tubular-formed region (cyan box) and tip region (red box) in the same root hair. (C) Recovery of fluorescence intensity for GFP-SYP123 and

(D) GFP-SYP132 after photo-bleaching was measured for 35 min, respectively, at the indicated time points.

Fig. 5. Effect of brefeldin A treatment on the localization of GFP-SYP123 and GFP-SYP132 in root hair cells. (A, B) 3D projection images of GFP-SYP123 and (C, D) GFP-SYP132. BFA treatment (20 μ M) induced large aggregations of GFP-SYP123 (B) but not GFP-SYP132 (D) inside root hairs. A and C represent mock (DMSO) controls. Scale bars = 20 μ m.

Fig. 6. mRFP-VAMP721/722/724 accumulate in the tip region of root hairs. (A, B) The root hair elongation zones of transgenic plants expressing mRFP-VAMP721, (C, D) mRFP-VAMP722, or (E, F) mRFP-VAMP724 were observed for the accumulation of fluorescence. Fluorescence accumulated in the tip region of root hairs from transgenic plants expressing mRFP-VAMP721, mRFP-VAMP 722, and mRFP-VAMP724. Scale bar = 10 μ m.

Fig. 7. SYP123 and SYP132 interact with VAMP721/722/724 *in vitro* and *in vivo*. (A) SYP123 forms SDS-resistant ternary SNARE complexes with SNAP33 and various VAMP 72 paralogs. (B) Interactions between SYP123 or SYP132 and VAMP721/722/723/724 *in vivo*. SYP123 and SYP132 fused to the N-terminal fragment of luciferase were co-expressed in protoplasts with

the indicated VAMPs conjugated to the C-terminal fragment of luciferase. Complemented luciferase activities were normalized to the activity of beetle red luciferase co-expressed in the protoplasts. Means and standard deviations were calculated from four independent biological replicates.

Fig. 8. Schematic model of the functional diversification of SYP123 and SYP132 in the growth of polarized root hair tips. We propose that *de novo* secretion of cell wall and plasma membrane materials is established by a SYP132 and VAMP721/722-mediated non-polar secretory pathway, followed by focal delivery of secretory vesicles to the root hair tip by an F-actin-dependent SYP123-mediated polarized recycling pathway, thereby tip-focused polarized secretion is established in root hair cells.

Supplementary Figure S1. Primary root lengths for WT and *syp123-1* mutant plants. The lengths of primary roots from 5-d-old WT and *syp123-1* seedlings were measured. Values represent mean \pm SD of 50 primary roots.

Supplementary Figure S2. The fluorescence images of a GFP-SYP132 expressing line crossed with a SYP132 amiRNA line. We crossed the GFP-SYP132-expressing line and the SYP132 amiRNA line. The F₁ generation of the crossed line was used for the observation. (A) GFP fluorescence was observed only in root hair cells in the presence of estradiol in a GFP/pER8GWExpA7 expressing plant. Scale bars =50 μ m. (B) Quantitative RT-PCR analysis of *SYP132* transcripts of 5-d-old seedlings of SYP132 amiRNA lines #1 and #2 in the presence or absence of 10 μ m estradiol. Polyubiquitin-10 gene (*UBQ10*) was used as an internal control. Values represent mean \pm SE (n=5). (C) The fluorescence of the root of GFP-SYP132 was observed in the presence of or absence of 10 μ m estradiol. White triangles indicate root hair cell files.

Supplementary Figure S3. Primary root lengths for SYP132 amiRNA plants. The lengths of primary roots from 5-d-old GFP and SYP132 amiRNA seedlings, in the presence or absence of estradiol, were measured. Values represent mean \pm SD of 50 primary roots. * $p < 0.01$, t-test.

Supplementary Figure S4. Effect of latrunculin B treatment on the localization of GFP-SYP132 in root hair cells. Scale bar = 20 μ m.

Supplementary Figure S5. Fluorescence images of GFP-SYP121 in the root hair of a transgenic plant ectopically expressing GFP-SYP121. (A) Projection of a growing root hair with polarized distribution of GFP-SYP121. (B) A growth-terminating root hair displaying a vanishing polarized distribution of GFP-SYP121. (C) Microscopic image of a growing root hair with its normal tip-focused GFP-SYP121 localization and (D) the corresponding density file (white = high fluorescence density, blue = low fluorescence density). (E) Microscopic image of a growing root hair after exposure to 1 μ M cytochalasin D and (F) the corresponding density profile. (G) The GFP-SYP121 transgenic plant was exposed to BFA.

Supplementary Figure S6. FRAP analysis of non-growing root hair. Images of GFP-SYP123 fluorescence before and after photo-bleaching. Before collecting the fluorescence images, photo-bleaching was performed around the root hair tip region. Fluorescence intensity was measured in the tubular-formed region (cyan box) and tip region (red box) in the same root hair.

Recovery of GFP-SYP123 fluorescence intensity after photo-bleaching was measured for 35 min at the indicated time points.

Supplementary Figure S7. Effect of tyrphostin A23 and A51 treatment on the localization of GFP-SYP123 in root hair cells. (A) GFP-SYP123 root hairs were treated with 50 μ M tyrphostin A23 and (B) A51. The arrow indicates the ruptured region. (C) Fluorescence intensity was measured for the indicated regions and (D, E) plotted at such times. Scale bar = 25 μ m.

Figure 1 Ichikawa et al.

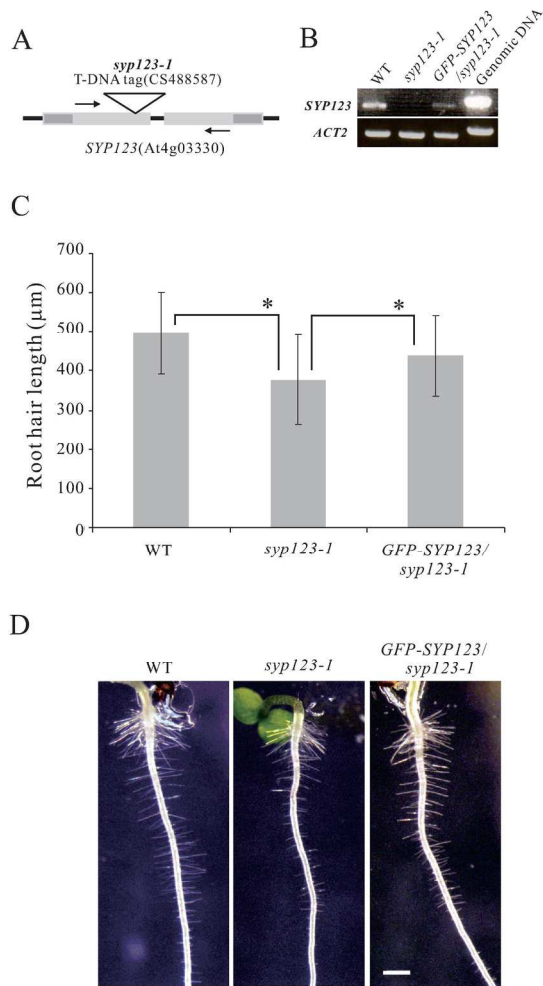


Fig. 1. The root hair elongation phenotype of the *syp123* mutant. (A) Schematic representation of SYP123 gene and the position of the T-DNA insertion. Boxes indicate exons. Dark grey regions indicate untranslated regions. The open triangle indicates the position of the T-DNA insertion. Arrows indicate the positions of primers used for RT-PCR and genomic PCR. (B) RT-PCR analysis to detect the expression of SYP123 in wild-type (WT) and mutant plants. Total RNA was purified from 7d-seedlings. ACT2 was used as an internal control. "Genomic DNA" indicates that PCR was performed by using Arabidopsis genomic DNA as a template. (C) Lengths of root hairs from WT, *syp123-1* mutant, and the complementation line expressing GFP-SYP123 under the control of its promoter in SYP123-1. Root hair length was measured using the 10 longest root hairs from 20 primary roots of 5-day-old each seedling on half-length MS agar plates. Values represent mean \pm SD of 200 root hairs. * $p < 0.01$, t-test. (D) Images of roots from WT, *syp123-1*, and GFP-SYP123/*syp123-1* plants. Scale Bar = 500 μ m.

173x228mm (300 x 300 DPI)

Figure 2 Ichikawa et al.

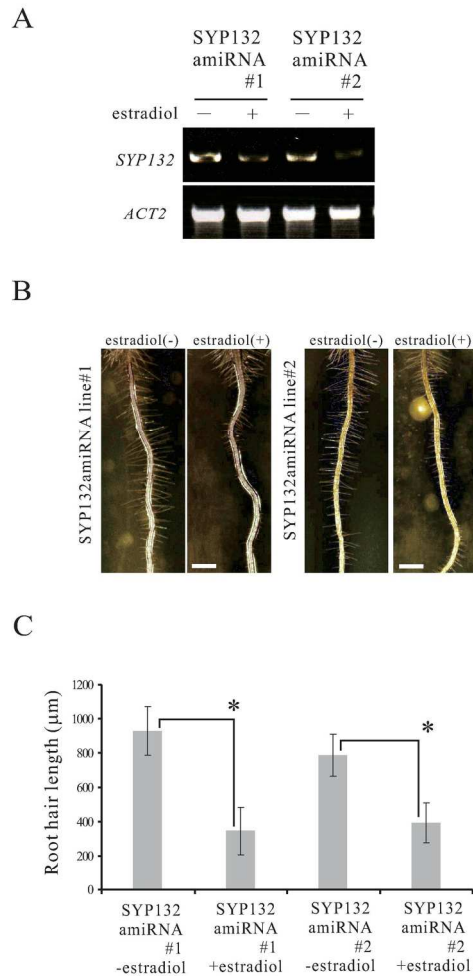


Fig. 2. The root hair elongation phenotype of SYP132 amiRNA plants. (A) RT-PCR analysis to detect the expression of SYP132 amiRNA plants (lines #1 and #2) and a GFP-expressing line in the presence or absence of 10 μ M estradiol. SYP132 in wild-type (WT) and mutant plants. ACT2 was used as an internal control. (B) Images of roots from SYP132 amiRNA plants (lines #1 and #2) in the presence or absence of estradiol. Scale bars = 1000 μ m. (C) The lengths of roots from SYP132 amiRNA plants in the presence or absence of 10 μ M estradiol. Root hair length was measured using the 10 longest root hairs from 20 primary roots of 5-day-old each seedling on half-length MS agar plates. Values represent mean \pm SD of 200 root hairs. * $p < 0.01$, t-test.
173x229mm (300 x 300 DPI)

Figure 3 Ichikawa et al.

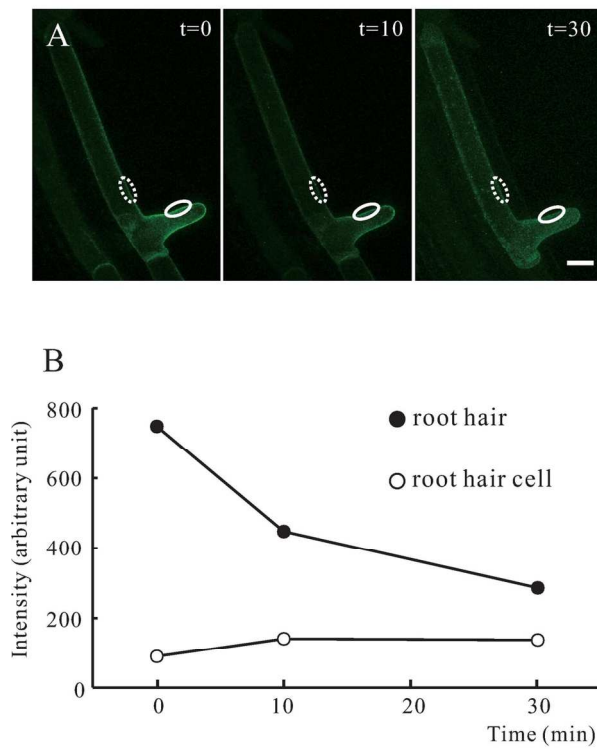


Fig. 3. Effect of latrunculin B treatment on the accumulation of GFP-SYP123 in the tip region of root hair cells. (A) Reconstituted 3D projection images of serial z-stack sections of root hair cells at the indicated times. GFP-SYP123 fluorescence immediately dispersed in the tip region of root hairs upon the addition of 2 μ M latrunculin B. (B) Quantitative analysis of signal intensity within the root hair cell (dotted circle) and root hair region (white circle) shown in (A). Scale bar = 20 μ m
152x182mm (300 x 300 DPI)

Figure 4 Ichikawa et al.

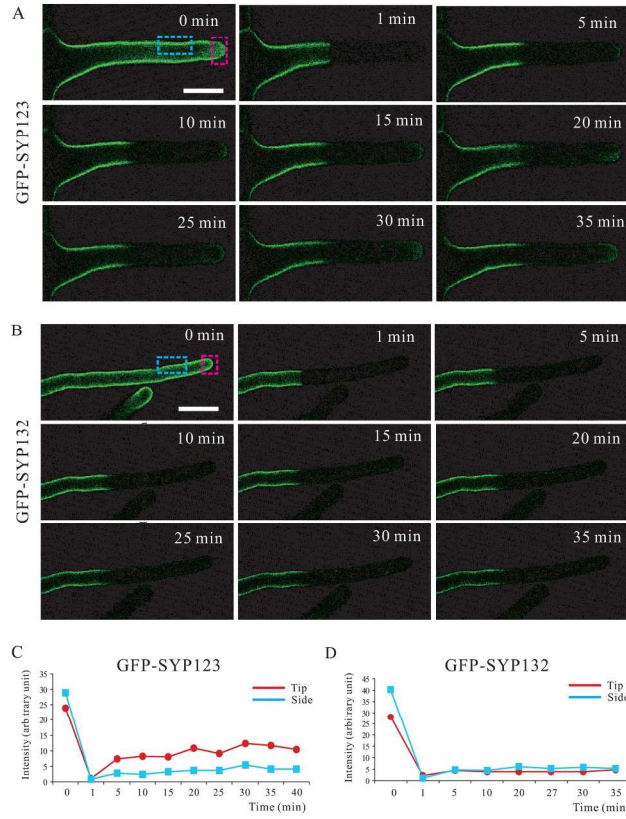


Fig. 4. FRAP analysis of GFP-SYP123 and GFP-SYP132. (A) GFP fluorescence images of GFP-SYP123 and (B) GFP-SYP132 before and after photo-bleaching. Before collecting the fluorescence images, photo-bleaching was performed around the root hair tip region. Fluorescence intensity was measured in the tubular-formed region (cyan box) and tip region (red box) in the same root hair. (C) Recovery of fluorescence intensity for GFP-SYP123 and (D) GFP-SYP132 after photo-bleaching was measured for 35 min, respectively, at the indicated time points.

210x184mm (300 x 300 DPI)

Figure 5 Ichikawa et al.

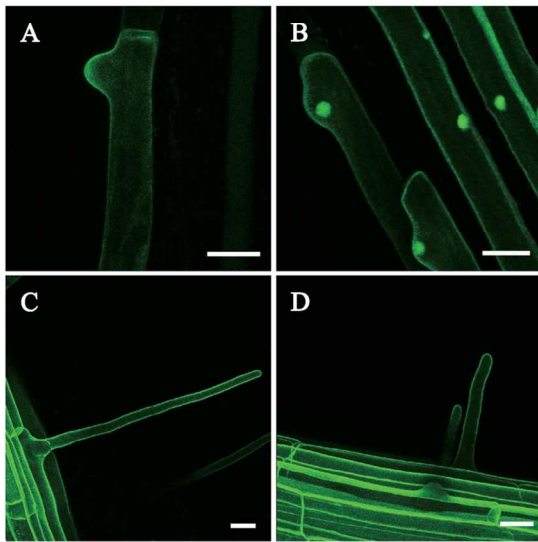


Fig. 5. Effect of brefeldin A treatment on the localization of GFP-SYP123 and GFP-SYP132 in root hair cells. (A, B) 3D projection images of GFP-SYP123 and (C, D) GFP-SYP132. BFA treatment (20 μ M) induced large aggregations of GFP-SYP123 (B) but not GFP-SYP132 (D) inside root hairs. A and C represent mock (DMSO) controls. Scale bars = 20 μ m.
123x115mm (300 x 300 DPI)

Figure 6 Ichikawa et al.

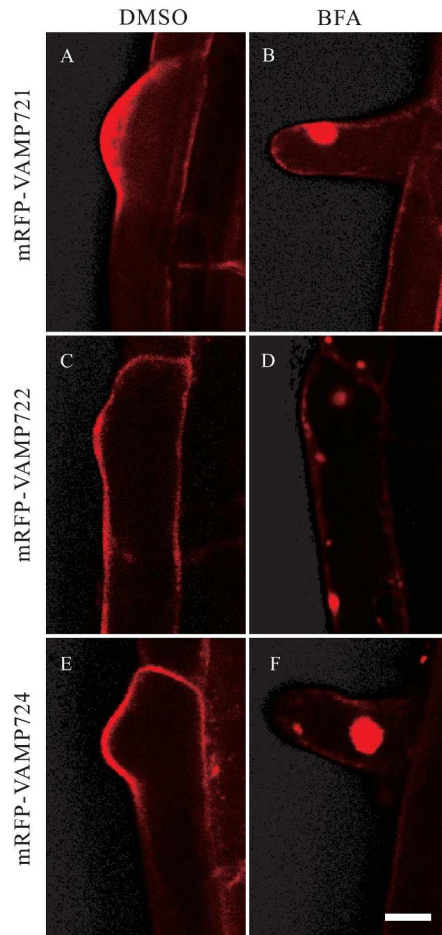


Fig. 6. mRFP-VAMP721/722/724 accumulate in the tip region of root hairs. (A, B) The root hair elongation zones of transgenic plants expressing mRFP-VAMP721, (C, D) mRFP-VAMP722, or (E, F) mRFP-VAMP724 were observed for the accumulation of fluorescence. Fluorescence accumulated in the tip region of root hairs from transgenic plants expressing mRFP-VAMP721, mRFP-VAMP 722, and mRFP-VAMP724. Scale bar = 10 μ m.

186x275mm (300 x 300 DPI)

Figure 7 Ichikawa et al.

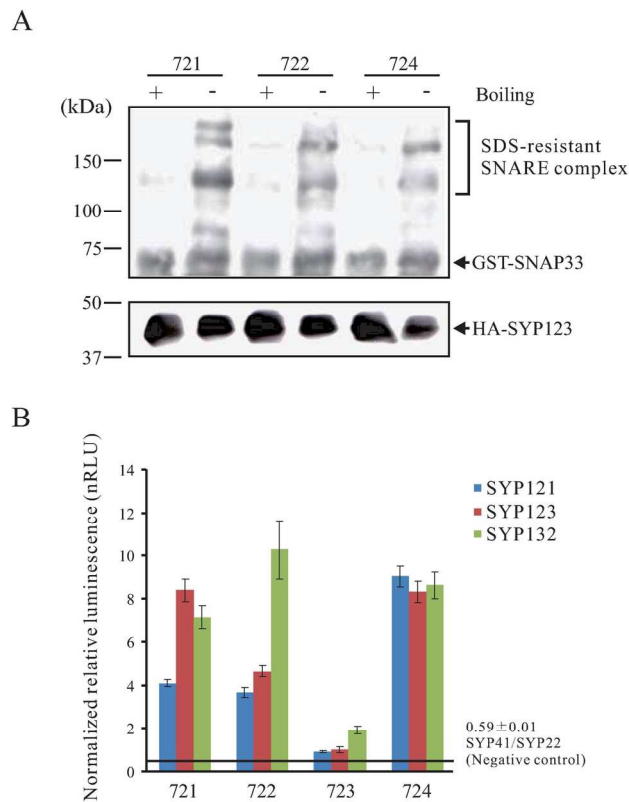


Fig. 7. SYP123 and SYP132 interact with VAMP721/722/724 in vitro and in vivo. (A) SYP123 forms SDS-resistant ternary SNARE complexes with SNAP33 and various VAMP 72 paralogs. (B) Interactions between SYP123 or SYP132 and VAMP721/722/723/724 in vivo. SYP123 and SYP132 fused to the N-terminal fragment of luciferase were co-expressed in protoplasts with the indicated VAMPs conjugated to the C-terminal fragment of luciferase. Complemented luciferase activities were normalized to the activity of beetle red luciferase co-expressed in the protoplasts. Means and standard deviations were calculated from four independent biological replicates.
163x185mm (300 x 300 DPI)

Figure 8 Ichikawa et al.

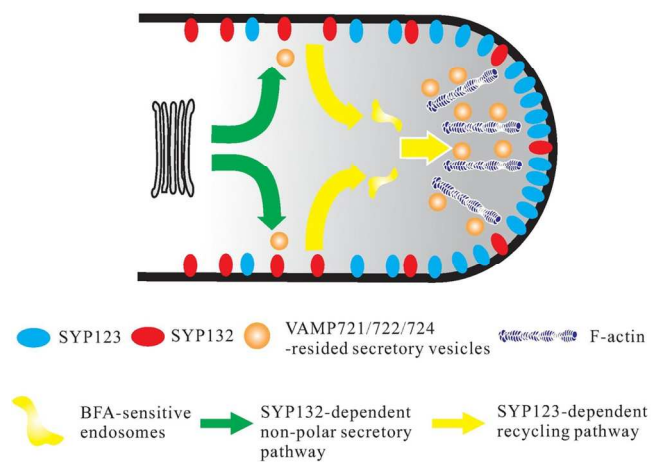


Fig. 8. Schematic model of the functional diversification of SYP123 and SYP132 in the growth of polarized root hair tips. We propose that de novo secretion of cell wall and plasma membrane materials is established by a SYP132 and VAMP721/722-mediated non-polar secretory pathway, followed by focal delivery of secretory vesicles to the root hair tip by an F-actin-dependent SYP123-mediated polarized recycling pathway, thereby tip-focused polarized secretion is established in root hair cells.
133x144mm (300 x 300 DPI)